Comparison of fully non-stationary artificial accelerograms generation methods in non-linear dynamic analyses

Federica Genovese[1,2,*], Giuseppe Muscolino[2], Alessandro Palmeri[1]
[1]*Loughborough University, United Kingdom, Email: {F.Genovese, A.Palmeri}@Lboro.ac.uk*
[2]*University of Messina, Italy, Email: {fedgenovese, gmuscolino}@unime.it*

Abstract: Non-linear dynamic analyses are a powerful tool to assess the performance of earthquake-resistant structural and geotechnical systems. Inevitably, the validity of the predicted seismic responses depends on the fidelity of the computational model to the true behaviour of the assets being analysed and the representativeness of time histories of ground acceleration in relation to the actual seismic hazard for the site under consideration. The generation of artificial time histories is generally allowed by international seismic codes and represents a valid alternative to the use of real accelerograms, provided that the key features in the expected seismic input are preserved in the generated signals. As a consequence, different stochastic generation methods of fully non-stationary, spectrum-compatible accelerograms have been proposed in the technical literature. The effects of two alternative randomisation strategies are compared in this paper, based respectively on the use of *i*) circular wavelet transform and *ii*) evolutionary piecewise power spectral density functions. The case of a simple nonlinear structural system with an elastoplastic behaviour is addressed, as representative of a broad range of structural and geotechnical systems that experience yielding and plastic deformations under relatively intense seismic events.

Keywords: Artificial accelerogram, Ground motion record, Inelastic response spectrum, Non-stationary stochastic process, Signal processing, Spectrum-compatible accelerogram, Wavelets transform.

1. Introduction

A proper definition of the design seismic action is a fundamental step in the dynamic analysis of structural and geotechnical systems as well as in dynamic soil-structure interaction problems. Seismic design codes typically represent the earthquake-induced ground shaking in terms of pseudo-acceleration response spectrum. However, there are situations (e.g. design of structures with passive protection devices or site response analysis) in which the use of the elastic design response spectrum is not considered appropriate and time-history analyses are required.

The increasing availability of strong motion records makes the use of real accelerograms an attractive option for defining the dynamic excitation. In this respect, the selection of representative sets of accelerograms is a crucial issue as it is influenced by multiple sources of uncertainties related to the definition of the seismic hazard at the site of interest. Different procedures for the selection of proper sets of recorded accelerograms have been proposed in the literature (e.g. Katsanos et al., 2010; Bommer and Acevedo, 2004). However, due to mechanical properties and non-linear behaviour of soils, there are situations in which it is not possible to obtain the minimum number of spectrum-compatible accelerograms required by seismic codes to carry out fully dynamic analysis without applying large scale factors to each record of the set, which may distort the recorded accelerogram, leading to unrealistic input motions (Genovese et al., 2019). In these situations, the use of artificial accelerograms could represent a possible alternative to realistically reproduce the seismic excitations. Since stationary artificial accelerograms are usually characterized by an excessive number of strong motion cycles and a high energy content, it becomes necessary to develop procedures to generate artificial accelerograms which suitably incorporate the large variability of the seismological parameters observed in real-life time-histories.

Over the years, procedures for the artificial generation of acceleration time histories have been proposed by several researchers. Saragoni and Hart (1974) simulates sample functions of a stochastic earthquake process, obtained by modulating contiguous regions of filtered Gaussian white noises using a deterministic time envelope function; Der Kiureghian and Crempien (1989) defined the generation process as a superposition of individually modulated stationary component processes, each representing the content in the motion in a distinct frequency band; Conte and Peng (1977) proposed a sigma oscillatory model in which each uniformly modulated process consists of the product of a real deterministic time modulating function and a stationary Gaussian sub-process.

This paper investigates two recently proposed methods for the simulation of artificial accelerograms, which both attempt to preserve the time variation of amplitude and frequency content of a target real strong motion record. The two alternative strategies are based respectively on the use of *i*) circular wavelet transform (*CWT*) and *ii*) evolutionary piecewise power spectral density (*EPSD*) function. In the first approach, the *CWT* method is used to decompose a real-valued parent (i.e. target) accelerogram into the superposition of complex-valued harmonic wavelets with complex-valued combination coefficients.

The second method, for a given target accelerogram, requires the following steps: *i*) to find a fully non-stationary model of earthquake ground motion such that the target accelerogram may be considered as one of its samples; *ii*) to evaluate the mean elastic spectrum of a set of generated fully non-stationary accelerogram samples; *iii*) to satisfy the compatibility with the elastic target response spectrum by means of an iterative procedure. In order to quantify the influence of these alternative probabilistic models on the seismic response of inelastic dynamic systems, constant-ductility response spectra have been computed for bilinear single-degree-of-freedom (SDoF) oscillators, considering different values of ductility.

2. Fully non-stationary generation methods

2.1. Wavelets formulation

The wavelet analysis consists in the expansion of a given signal in terms of "wavelets" which are generated by scaling and shifting a fixed function called "mother wavelet". Among all different types of wavelets, the "harmonic wavelets" and "musical wavelets" proposed by Newland (1994) are particularly useful for dynamic analysis. These families of wavelets are complex-valued functions in the time domain, with a rectangular box-shaped Fourier transform in the frequency domain.

Another approach to decompose the real-valued signal $\ddot{U}_{\mathrm{g}}(t)$ into the superposition of complex-valued wavelets $\psi_{\{m,n\},k}(t)$ having complex-valued combination coefficients $a_{\{m,n\},k}$ consists in the use of the circular wavelets:

$$\psi_{\{m,n\},k}(t) = \frac{1}{n-m} \sum_{j=m}^{n-1} \exp\left[\mathrm{i}\, 2\pi j \left(t - \tau_{\{m,n\},k} \right) \right] \tag{1}$$

where $\tau_{\{m,n\},k} = k/(n-m)$ is a deterministic time shift of the wavelets belonging to the $\{m,n\}-$ indexed frequency band, while k is an integer number.

In the discrete wavelets transform, the complex-valued combination coefficients $a_{\{m,n\},k}$ of the parent function are calculated by a discrete convolution of the signal $\ddot{U}_{\mathrm{g}}(t)$ with the band wavelets $\psi_{\{m,n\},k}(t)$ (Cecini and Palmeri, 2015):

$$a_{\{m,n\},k} = \sum_{\ell=0}^{N} \ddot{U}_{\mathrm{g}}\left(\frac{t_\ell}{t_f}\right) \cdot \frac{\Delta t}{t_f} \cdot \psi_{\{m,n\},k}\left(t_\ell\right) \tag{2}$$

where k =0, ..., (n-m-1), $t_\ell = \ell \cdot \Delta t$ is the ℓth of the $N = t_f / \Delta t$ discrete time instants at which the signal is discretized, being Δt and t_f the sampling interval and the time duration of the signal, respectively.

In this paper, the randomisation of the target signal $\ddot{U}_{\mathrm{g}}(t)$ has been evaluated using the circular wavelet as mother wavelet.

The generation formula for the rth sample of the random process can be written as:

$$f^{(r)}(t) = 2\sum_{\{m,n\}} \sum_{k=0}^{n-m-1} \sum_{j=m}^{n-1} \frac{\left|a_{\{m,n\},k}\right|}{n-m} \times \cos\left[\mathrm{i}\, 2\pi j\left(t-\tau_{\{m,n\},k}\right) + \theta_{\{m,n\},k} + \phi^{(r)}_{\{m,n\},k}\right] \tag{3}$$

where $\phi^{(r)}_{\{m,n\},k}$ is the rth realization of a random variable uniformly distributed over the interval $\left[0, 2\pi\right]$ while $\bar{\theta}_{\{m,n\},k} = \arg\left\{\bar{a}_{\{m,n\},k}\right\}$ is the corresponding deterministic phase of the complex-valued coefficient of the parent signal.

2.2. EVOLUTIONARY POWER SPECTRAL DENSITY FUNCTION METHOD

According to the model proposed by Muscolino et al. (2021), the second method for generating random samples of a fully non-stationary zero-mean Gaussian process considered in this paper, consists of a four-step procedure.

First, divide the time axis of the target accelerogram in n contiguous time intervals, in which a uniformly modulated process is introduced as the product of a deterministic modulating function, $a(t)$, times a stationary zero-mean Gaussian sub-process $X_k(t)$, whose power spectral density (PSD) function $G_{X_k}(\omega)$ is filtered by two Butterworth filters:

$$G_{X_k}(\omega) = \beta_k \left(\frac{\omega^2}{\omega^2 + \omega_{H,k}^2}\right)\left(\frac{\omega_{L,k}^4}{\omega^4 + \omega_{L,k}^4}\right)\frac{\rho_k}{\pi}\left(\frac{1}{\rho_k^2 + (\omega+\Omega_k)^2} + \frac{1}{\rho_k^2 + (\omega-\Omega_k)^2}\right); \quad k = 1,\dots,n \tag{4}$$

where β_k is evaluated in such a way that the sub-process $X_k(t)$ possesses unit variance. All the parameters present in Eq. 4 depend on the occurrences of maxima P_k and of zero-level up-crossings $N^+_{0,k}$ of the target accelerogram, in the various k intervals:

$$\Omega_k \cong \frac{2\pi N_{0,k}^+}{\Delta T_k}; \quad \rho_k \simeq \frac{\pi N_{0,k}^+}{2\Delta T_k}\left[\pi - 2\frac{N_{0,k}^+}{P_k}\right] \tag{5}$$

Second, estimate, in each time interval, the parameters of modulating function $a(t)$ by least-square fitting the expected energy of the proposed model to the energy of the target accelerogram subdivided in three parts:

$$a(t)=\sum_{j=1}^{2}\bar{a}_j(t)\,\mathbb{W}(t_{j-1},t_j)+a(t_2)\exp\left[\frac{(t-t_2)}{T_D-t_2}\ln\left(\frac{\left|\ddot{U}_{\mathrm{g}}(T_f)\right|}{a(t_{n_a-1})}\right)\right]\mathbb{W}(t_2,t_3), \tag{6}$$

in which $\mathbb{W}(t_{k-1},t_k)=\mathbb{U}(t-t_k)-\mathbb{U}(t-t_{k-1})$ is the window function, $\mathbb{U}(t)$ being the unit step function.

Third, generate the ith sample of the process via the formula:

$$F_0^{(i)}(t)=a(t)\sqrt{2\Delta\omega}\left[\sum_{k=1}^{n}\sum_{r=1}^{m_N}\mathbb{W}(t_{k-1},t_k)\sin\left(r\,\Delta\omega t+\theta_r^{(i)}\right)\sqrt{G_{X_k}\left(r\,\Delta\omega\right)}\right] \tag{7}$$

$\theta_r^{(i)}$ being the random phase angles, uniformly distributed over the interval $\left[0,2\pi\right]$; m_N is the number of parts in which the *PSD* function is discretized while $\Delta\omega$ is the frequency sampling interval.

Lastly, reduce the gap between the elastic response spectrum of target accelerogram $S_e^{(T)}$ and the mean elastic response spectrum of artificial accelerograms $\bar{S}_e^{(j-1)}$ through the introduction of a corrective iterative *PSD* function:

$$\bar{G}_{X_k}^{(j)}(\omega_k)=\bar{G}_{X_k}^{(j-1)}(\omega_k)\,\frac{S_e^{(T)}(\omega_\ell,\zeta_0)^2}{\bar{S}_e^{(j-1)}(\omega_\ell,\zeta_0)^2}$$

being $\bar{G}_0^{(0)}(\omega_k)=1$ in the first iteration Vanmarcke and Gasparini (1977).

According to the formulation described by Genovese et al. (2020), a set of samples can be generated as:

$$\bar{F}_0^{(i)}(t)=a(t)\sqrt{2\Delta\omega}\left[\sum_{k=1}^{n}\sum_{r=1}^{m_N}\mathbb{W}(t_{k-1},t_k)\sin\left(r\,\Delta\omega t+\theta_r^{(i)}\right)\sqrt{\bar{G}_0^{(j)}(r\,\Delta\omega)G_{X_k}\left(r\,\Delta\omega\right)}\right]. \tag{8}$$

3. Numerical application

In order to highlight the performance of the two proposed procedures to generate sets of accelerograms having main characteristics similar to those of the target one, and consequently useful for the non-linear time-histories analysis, constant ductility response spectra have been computed for bilinear and stiffness degrading load-deformation models, considering different displacement ductility values.

3.1. Target Motion

The North-South component of the ground motion recorded at Vasquez Rocks Park during the 1994 Northridge earthquake has been downloaded from the PEER database (Ancheta et al., 2013) and has been used in the following as target accelerogram. The selected ground motion, with Moment Magnitude $M_w = 6.7$ and a site-source distance $R_{JB} = 23.1$ km (Joyner and Boore, 1979), has been recorded by a station with an average shear wave velocity in the upper 30 m equal to $V_{s,30} = 996$ m/s (EC8, soil class "A"). The target accelerogram, having an overall duration $T_f = 36.6$ s and a sampling interval $\Delta t = 0.02\,\text{s}$, is characterized by a peak ground acceleration $a_{max} = 0.132\ g$, a total and Arias intensity equal to $I_0 = 1.9$ m^2/s^3 and $I_A = 0.3$ m/s, respectively, and a total number of zero-level up-crossings and of peaks equal to $N_0^+ = 196$ and $P_0 = 212$, respectively. The recommended lowest usable frequency related to the filtering of the target record to remove low-frequency (long-period) noise is equal to 0.25 Hz.

3.2 Wavelets-based method

Due to the Heisenberg's uncertainly principle, it is not possible simultaneously localize a signal in both the time and frequency domains (Mallat, 2009).

In this paper, three different schemes of Circular Wavelet Transform (*CWT*) have been investigated to highlights how the trade-off between localizations in the two domains plays a fundamental role for the purpose of generating meaningful time histories of ground accelerations.

The three different configurations correspond to p=1, 32 and 915 frequency bands of equal bandwidth, and 50 acceleration time-histories have been generated by Eq. (3). Three generic samples together with the target accelerogram (black line) are plotted in Figure 1.

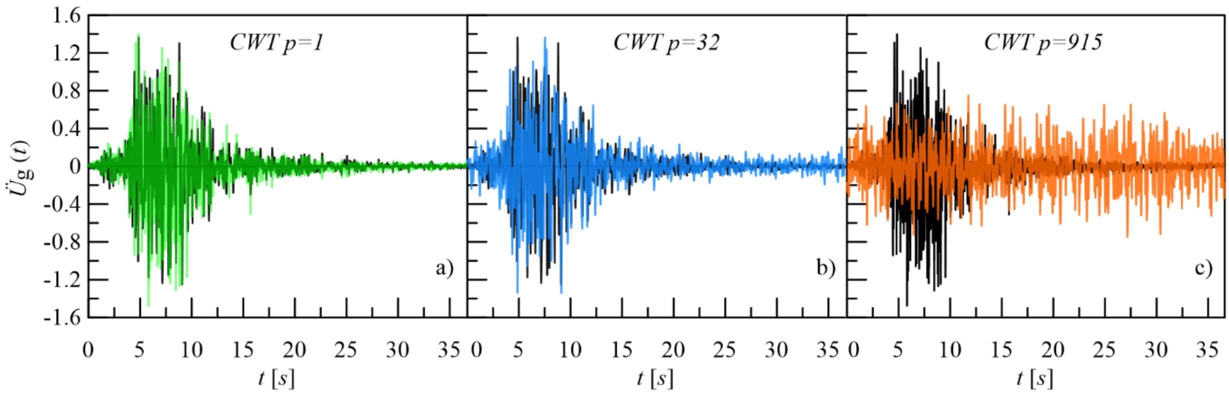

Figure 1. Comparison among the selected accelerogram (black line) and the *i*th generated sample by the proposed circular wavelets method, considering a subdivision of the frequency domain into a) p=1 (green line), b) p=32 (blue line) and c) p=915 (orange line), frequencies bands.

As the number of bands increase, the fidelity in representing the frequency content is increases but at the same time the generated samples tend to lose the fidelity in terms of non-stationary characteristics, until they become realizations of a stationary random process (see Figure 1c, with p= 915). This effect is also highlighted in Figure 2 in which the mean values of the modules of the Fourier spectra, obtained for the three analysed configurations, are compared with the target one.

In Figures 3a and 3b, a further comparison is represented in terms of cumulative energy functions $I_0(t)$ and cumulative zero-level up crossing functions $N_0^+(t)$, respectively. For *p*=1, the mean trend of the energy function is in a good agreement with the target one (dashed black line) while the zero-level up crossing function is very far from the real trend. The opposite happens in the third case, *p*=915.

Consequently, it is necessary to find, a central configuration between the 2 extreme cases, to obtain samples having characteristics sufficiently close to those of the target one both in the time and frequency domain. The case of *p*=32 allows to obtain a result, with a sufficient degree of accuracy, in both domains.

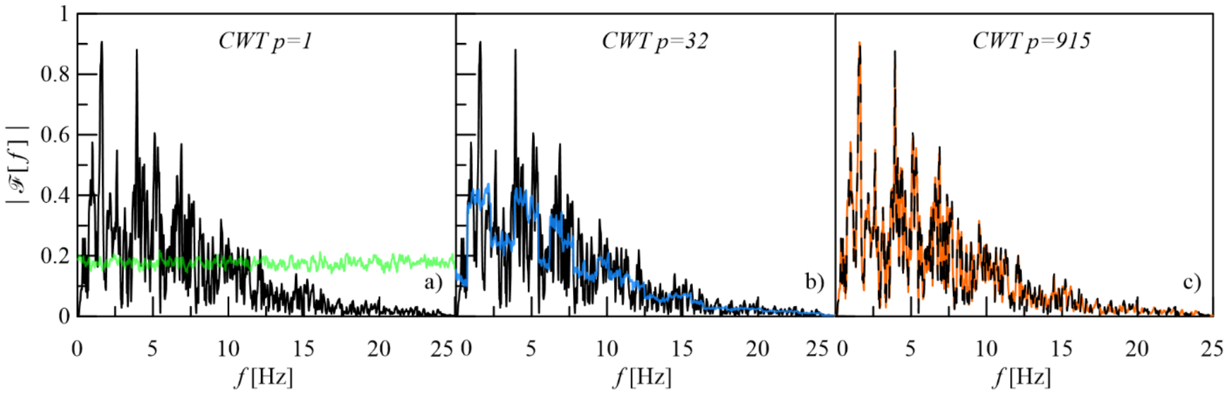

Figure 2. Comparison among the target Fourier spectrum module (black line) and the *i*th Fourier spectrum module of the generated sample by the *CWT* method, considering a) *p*=1 (green line), b) *p*=32 (blue line) and c) *p*=915 (orange line) frequencies bands.

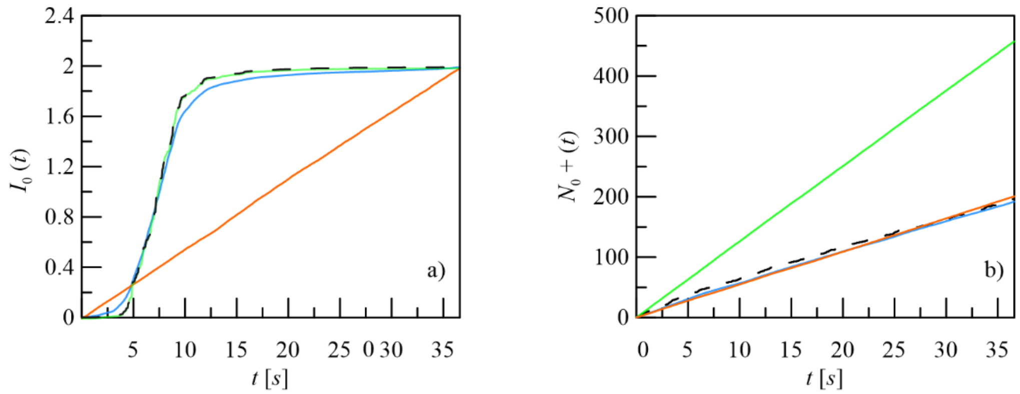

Figure 3. Comparison between the target (black, dashed lines) and the averages a) cumulative energy functions, b) zero level up crossing functions, considering *p*=1 (green lines), *p*=32 (blue lines) and *p*=915 (orange lines) frequencies bands.

3.3 EVOLUTIONARY POWER SPECTRAL DENSITY FUNCTION (*EPSD*) METHOD

Using the iterative procedure described in Section 2.2, a set of 50 artificial accelerograms, after 4 iterations, has been generated using appropriate modulating and *PSD* functions which allowed to preserve the amplitude and the frequency content of the target ground motion. Further details about the parameters that characterize these functions can be found in (Genovese et al., 2020).

3.4. NON-LINEAR DYNAMIC ANALYSES

In this section, inelastic response spectra have been computed to reproduce actual nonlinear structural response by means of an elastoplastic representation of a SDoF oscillator.

Specifically, the post-yield kinematic hardening ratio has been set equal to 0, i.e. an elastic-perfectly plastic system has been analyzed.

All the spectra have been obtained using the SeismoSpect 2021 Software, with a linear baseline correction, for a 2% damping value and three different ductility factors μ equal to 2, 5, and 8, respectively.

In Figure 4, the velocity spectra of the target accelerogram (red lines) are compared to that obtained as the mean value of 50 samples (black continues lines), for μ=5, considering the three different schemes analysed with the Circular Wavelet Transform method and samples generated by the Evolutionary Power spectral density function method.

The confidence intervals evaluated as the means values plus/minus the corresponding standard deviations (black dotted lines) and the velocity spectra of each sample (gray lines) are also reported in Figure 4.

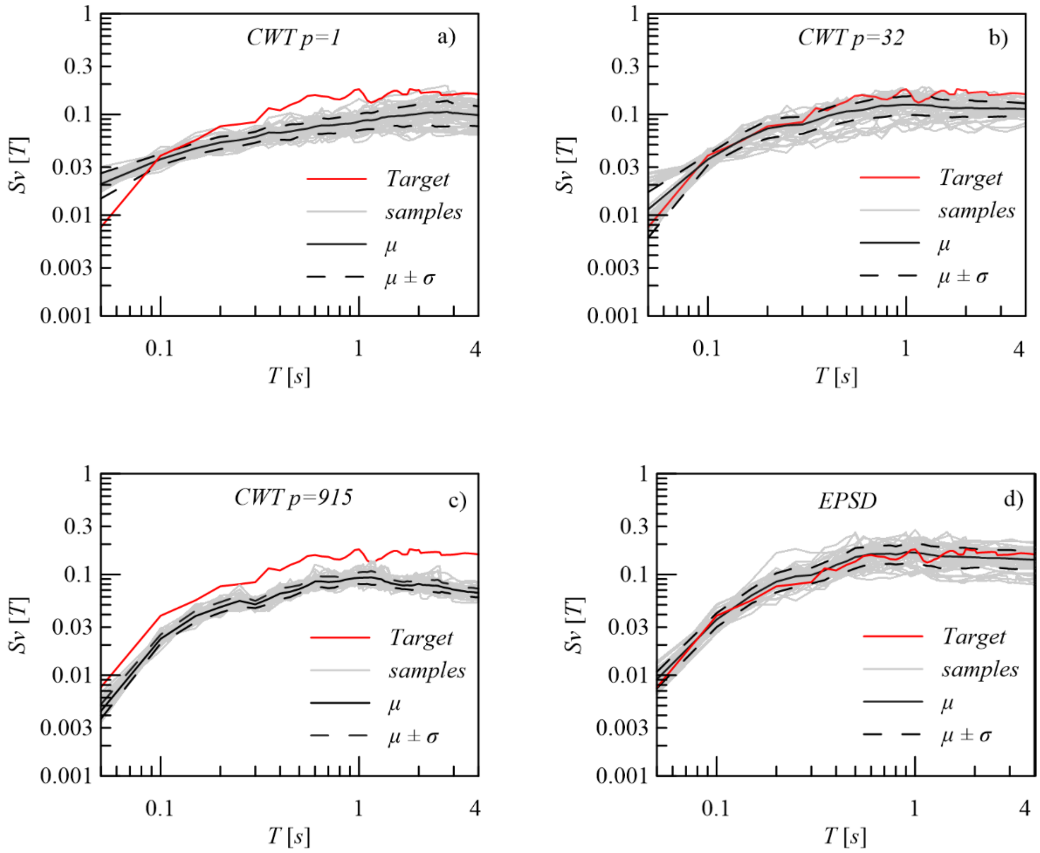

Figure 4. Comparison among the target velocity spectrum (red line) and the mean one (black, continue line), of the generated samples (gray lines) together with the corresponding mean value plus/minus standard deviation functions (black dashed lines) for a) *p*=1, b) *p*=32, c) *p*=915 frequencies bands, d) *EPSD* function method.

A comparison between the mean inelastic velocity spectra of the generated samples by *CWT* transform method (case p=32) and by the *EPSD* function one, for three different ductility factors, are shown in Figure 5a and b, respectively.

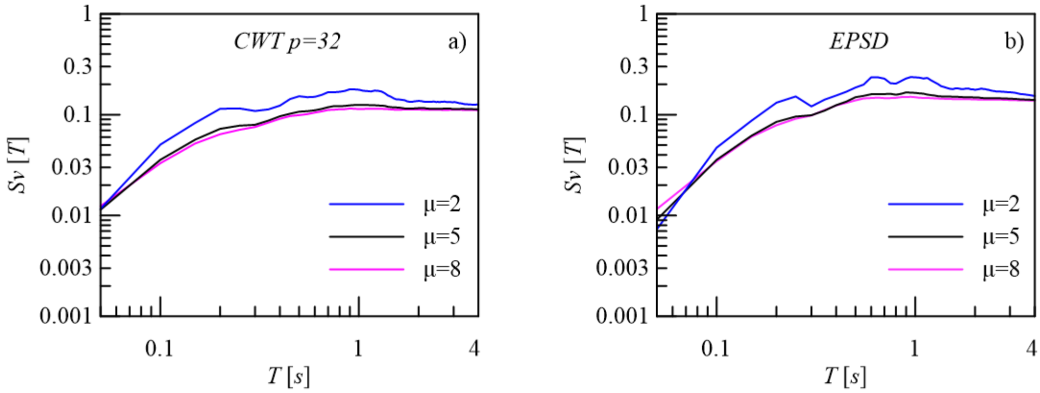

Figure 5. Comparison between mean velocity spectra evaluated for different ductility factors: a) *CWT* method p=32, b) *EPSD* function method.

Conclusions

In this paper, two recently proposed methods for generating samples of fully non-stationary zero-mean Gaussian processes, having a target acceleration time-history as one of its own samples, have been compared.

The *CWT*-method, consisting of a phase angle rotation of the circular wavelets, allows generating the required number of fully non-stationary samples without the need of defying the evolutionary power spectral density function of the ground acceleration.

The correct choice of the number of bands in which to divide the frequency domain is an important step to generate samples with the desired time-variation of amplitude and frequency content.

Further work may be needed to optimize the selection of the frequency bands, e.g. with non-uniform bandwidths.

The *EPSD* function method allows to obtain samples with characteristics closer to the target event than those generated with *CWT* method. However, the latter procedure tends to be more complex and requires several iterative steps.

The numerical results show that the average values of the inelastic velocity spectra of the generated, samples obtained by the *CWT* method, are close to the target one in the case of the subdivision of the frequency domain in 32 parts.

The other 2 configurations studied lead to results totally different from the real one. This is due to the loss of fidelity in wither the time or frequency domain, thus confirming the importance of accurately representing the seismic input in both domains.

By contrast, the application of iterative corrections in the *EPSD* method allows the target velocity spectrum to completely fall into the confidence interval evaluated as the mean value plus/minus standard deviation of the velocity spectrum of the generated samples.

References

Ancheta, T.D. et al. *PEER NGA-West2 database*. Pacific Earthquake Engineering Research Center/03; California; 2013.

Bommer, J.J. and B. Acevedo. The use of real earthquake accelerograms as input to dynamic analysis. *Journal of Earthquake Engineering*, 8, Special issue, 1, pp. 43-91. 2004

Cecini, D. and A. Palmeri. Spectrum-compatible accelerograms with harmonic wavelets. *Computers and Structures*. Vol. 147, pp.26-35, 2015.

Conte, J.P., Peng, B.-F. (1997). Fully nonstationary analytical earthquake ground-motion model. *Journal of Engineering Mechanics* (ASCE), 123(1), pp. 15-24, 1997.

Der Kiureghian A. and J. Crempien J. An evolutionary model for earthquake ground motion. *Structural Safety*, 6 , pp. 235-246, 1989.

Genovese, F., D., Aliberti, G. Biondi and E. Cascone. A procedure for the selection of input ground motion for 1D seismic response analysis. Earthquake Geotechnical Engineering for Protection and Development of Environment and constructions – Silvestri and Moraci (Eds). *Proceedings of the 7th ICEGE*, 17-20 June 2019, Rome, Italy, pp. 2591-2598, 2019.

Genovese, F., G. Muscolino, G. Biondi and E. Cascone. Generation of artificial accelerograms consistent with earthquake-induced ground motions. *Proceedings of the 11th International Conference on Structural Dynamic*, EURODYN, Virtual, Athens; Greece; 23-26 November 2020; Code 165382, Vol. 2, Pages 3027-3042, 2020.

Joyner, W.B., and D.M. Boore. Peak horizontal acceleration and velocity from strong motion records including records from the 1979 Imperial Valley, California, earthquake. *Bulletin of the Seismological Society of America* 1981; 71: 2011–2038.

Katsanos, E.I., A.G. Sextos and G.D. Manolis. Selection of earthquake ground motion records: A state-of-the-art review from a structural engineering perspective 2010. *Soil Dynamics and Earthquake Engineering*, 30 (4), pp. 157-169, 2010.

Mallat, S. A Wavelet tour of signal processing: the sparse way. *Elsevier, Academic*, 2009.

Newland D. Harmonic and musical wavelet. *Proceedings. Royal Society A*, Vol. 444, pp.605-620, 1994.

Muscolino, G., F. Genovese, G. Biondi and E. Cascone. Generation of Fully Non-Stationary Random Processes Consistent with Target Seismic Accelerograms. *Soil Dynamics and Earthquake Engineering*, 141(106467):1-14, 2021.

Saragoni, G. R. and G.C. Hart. Simulation of earthquake ground motions. *Earthquake engineering and structural dynamics*, 2, pp. 249-267, 1974.

SeismoSpect. *Seismosoft: Earthquake engineering software products*, 2021.

Vanmarcke, E.H. and D.A. Gasparini. Simulated earthquake ground motions. *Proceedings SMIRT-4 Conference*, San Francisco, paper K1/9, 1977.